Reduced interface recombination in Cu2ZnSnS4 solar cells with atomic layer deposition Zn1−xSnxOy buffer layers

C. Platzer-Björkman, C. Frisk, J. K. Larsen, T. Ericson, S.-Y. Li, J. J. S. Scragg, J. Keller, F. Larsson, and T. Törndahl

Citation: Applied Physics Letters **107**, 243904 (2015); doi: 10.1063/1.4937998
View online: http://dx.doi.org/10.1063/1.4937998
View Table of Contents: http://scitation.aip.org/content/aip/journal/apl/107/24?ver=pdfcov
Published by the AIP Publishing

Reduced interface recombination in Cu_2ZnSnS_4 solar cells with atomic layer deposition $Zn_{1-x}Sn_xO_y$ buffer layers

C. Platzer-Björkman, C. Frisk, J. K. Larsen, T. Ericson, S.-Y. Li, J. J. S. Scragg, J. Keller, F. Larsson, and T. Törndahl
Ångström Solar Center, Solid State Electronics, Engineering Sciences, Uppsala University, Box 534, 75121 Uppsala, Sweden

(Received 19 October 2015; accepted 28 November 2015; published online 14 December 2015)

Cu_2ZnSnS_4 (CZTS) solar cells typically include a CdS buffer layer in between the CZTS and ZnO front contact. For sulfide CZTS, with a bandgap around 1.5 eV, the band alignment between CZTS and CdS is not ideal ("cliff-like"), which enhances interface recombination. In this work, we show how a $Zn_{1-x}Sn_xO_y$ (ZTO) buffer layer can replace CdS, resulting in improved open circuit voltages (V_{oc}) for CZTS devices. The ZTO is deposited by atomic layer deposition (ALD), with a process previously developed for $Cu(In,Ga)Se_2$ solar cells. By varying the ALD process temperature, the position of the conduction band minimum of the ZTO is varied in relation to that of CZTS. A ZTO process at 95 °C is found to give higher V_{oc} and efficiency as compared with the CdS reference devices. For a ZTO process at 120 °C, where the conduction band alignment is expected to be the same as for CdS, the V_{oc} and efficiency is similar to the CdS reference. Further increase in conduction band minimum by lowering the deposition temperature to 80 °C shows blocking of forward current and reduced fill factor, consistent with barrier formation at the junction. Temperature-dependent current voltage analysis gives an activation energy for recombination of 1.36 eV for the best ZTO device compared with 0.98 eV for CdS. We argue that the V_{oc} of the best ZTO devices is limited by bulk recombination, in agreement with a room temperature photoluminescence peak at around 1.3 eV for both devices, while the CdS device is limited by interface recombination.
[http://dx.doi.org/10.1063/1.4937998]

Thin film solar cells based on Cu_2ZnSnS_4 (CZTS) are attractive alternatives to CdTe and CIGS solar cells since only highly abundant elements are used. The material has been intensively studied following initial investigations by Ito and Nakazawa[1] and Katagiri[2] where gradual efficiency improvements have led to efficiencies of up to 12.6% for selenium containing CZTS.[3] The main efficiency limitation for record CZTS devices is the open circuit voltage, V_{oc}. Several reasons for the large V_{oc} deficit (of around 840 mV for sulfide CZTS[4]) in relation to the band gap have been suggested. One is an unfavorable alignment of the conduction band minima (CBM) at the CZTS/CdS interface, where CdS has a lower CBM as compared with CZTS.[5] This type of interface (a so-called "cliff") will lead to increased interface recombination and losses in V_{oc}.

The most frequently used method for determining the dominating recombination path is temperature dependent current voltage analysis, JVT. Provided that the ideality factor shows no significant temperature dependence, this method allows for the determination of the activation energy of the dark saturation current, which in turn depends on the dominating recombination path.[6,7] The standard interpretation is that an activation energy equal to the band gap is compatible with bulk recombination being dominant, while an activation energy lower than the band gap indicates that interface recombination is limiting V_{oc}. For most CZTS devices, including record devices, JVT analysis yields activation energies below the band gap energy. Only in some cases of pure selenide CZTSe, activation energies of 1 eV, i.e., the bulk band gap, have been obtained.[8] The reason for the better performance of selenium rich, low band gap, CZTSe as compared with sulfur rich CZTS could be either a more beneficial energy band alignment at the CdS/CZTSe interface, or higher electronic quality of the bulk material.

In this work, we investigate an alternative buffer layer for pure sulfide CZTS solar cells, replacing CdS with a $Zn_{1-x}Sn_xO_y$ (ZTO) buffer layer grown by atomic layer deposition (ALD). For CIGS solar cells, the conduction band offset (CBO) of a $Zn_{0.8}Sn_{0.2}O_y$ buffer layer deposited at 120 °C has been estimated to be +0.1 eV towards CIGS with a surface band gap of 1.15 eV by using synchrotron x-ray techniques.[9] This CBO is similar to reported values for the CdS/CIGS interface.[10] In a previous study, it was shown that the band gap of ZTO increases as a function of decreasing deposition temperature, due to quantum confinement effects.[11] The detected change in band gap energy mainly affects the position of the conduction band edge in ZTO, where an ALD deposition temperature of 90 °C displayed a widening of the ZTO band gap by 0.25 eV, leading to a blocking behavior in CIGS solar cells.[12] From the ZTO/CIGS data, an optimal CBO for ZTO/CZTS is estimated to be obtained at a deposition temperature of 95 °C. We now apply this buffer layer to CZTS and study the influence of deposition temperature on device performance, V_{oc} deficit, and JVT behavior, and show strong improvements in V_{oc} with the alternative buffer layer.

TABLE I. IV parameters for average or (best) device with different buffer layers or CZTS surface treatments. The number of ALD cycles is 800 for A1-3, 730 for B1, and 1100 for B2.

Sample	Process (total # of cells)	Sn/Sn + Zn	Thickness (nm)	V_{oc} (mV)	J_{sc} (mA/cm^2)	FF (%)	Eff. (%)
A1	KCN + ALD 95 °C (8)	0.17	40	690 (687)	17.5 (17.7)	49.6 (58.3)	6.0 (7.1)
A1	2 min light-soaking (1)	0.17	40	682	17.9	60.2	7.4
A2	Water + ALD 95 °C (6)	0.17	40	658 (661)	17.8 (18.2)	55.1 (56.6)	6.4 (6.8)
A3	ALD 95 °C (6)	0.17	40	635 (647)	13.6 (13.9)	38.6 (40.4)	3.4 (3.6)
A_{ref}	CdS (8)	…		584 (607)	17.1 (17.1)	52.6 (55.9)	5.3 (5.8)
B1	KCN ALD 120 °C (4)	0.24	74	677 (676)	18.7 (18.8)	51.2 (53.2)	6.5 (6.8)
B2	KCN ALD 80 °C (7)	0.26	98	706 (713)	17.9 (18.1)	40.6 (42.1)	5.1 (5.4)
B_{ref}	CdS (3)	…		641 (666)	20.9 (19.4)	46.9 (55.6)	6.2 (7.2)

CZTS absorbers are grown on soda lime glass with 300 nm Mo deposited by DC sputtering. CZTS precursor films are deposited by reactive sputtering from CuS, Zn, and Sn targets in mixed Ar:H_2S at a substrate temperature of 180 °C as described in Ref. 13. Two series of devices with different buffer layer processes are made as shown in Table I. In batch A, precursor films with Cu/Sn ratio of 1.86 and Zn/(Cu + Sn) = 0.45 are used and in batch B the composition is Cu/Sn = 1.95 and Zn/Cu + Sn = 0.35. Annealing is performed in a tube furnace with background pressure of 350 mbar of argon, where the samples are loaded into a graphite box with around 30 mg of sulfur. In each annealing run, four $2.5 \times 2.5\,cm^2$ sized samples are loaded. The box is inserted into a hot zone giving rapid heating of the sample up to 560 °C, followed by a 10 min dwell after which the box is removed from the hot zone to cool down. After unloading, reference devices are fabricated from one of the four samples by etching in 5% KCN solution for 2 min followed by chemical bath deposition of CdS, RF sputtering of ZnO/ZnO:Al bilayer, Ni/Al/Ni grid by e-beam evaporation, and mechanical scribing of six to eight $0.5\,cm^2$ cells according to the Ångström Solar Center baseline procedure.[14] Devices with ALD buffer layers are etched with 5 wt. % KCN, except for A2 and A3 in Table I, where a comparison with pure water dipping and unetched (as deposited) CZTS was made. These tests showed the highest performance for KCN etching and therefore alternative interface treatments were not studied further. After etching, rinsing, and drying, CZTS absorbers are loaded into a Microchemistry F-120 reactor and heated to the reaction temperatures of 80, 95, or 120 °C for 30 min. The ZTO buffer layers are grown by using N_2 as a carrier gas, and diethyl zinc [$Zn(C_2H_5)_2$], tetrakisdimethylaminotin(IV) [$Sn(N(CH_3)_2)_4$], and deionized water as precursors.[15] A Sn/(Sn + Zn) precursor pulse ratio of 0.5 is used, where the length of the Sn/Zn precursor:N_2:H_2O:N_2 pulses are 400/400:800:400:800 ms, respectively. Cycling is always terminated by the water pulse, and started by a zinc precursor pulse. The ZTO is confirmed to be conformally covering the CZTS, as expected, by transmission electron microscopy. Device finishing is done with the same ZnO/ZnO:Al, grid, and scribing as for CdS reference devices. Dark and illuminated JV measurements are performed in a class A solar simulator from Newport. External quantum efficiency (QE) is measured in a homebuilt setup calibrated with external Si calibration cells from Hamamatsu. JVT measurements are performed in a cryostat connected to a liquid nitrogen source and a Lakeshore 220 autotuning temperature controller. JVT is done using a Keithley 2041 SourceMeter under white light LED, adjusting the current to the lamp to match the J_{sc}. PL measurements are performed in a Renishaw inVia confocal Raman microscope equipped with a silicon CCD detector. All measurements are performed at room temperature, using a 532 nm laser and an excitation intensity of about 1300 W/cm^2. The measurements are corrected for the system spectral response using an Avantes calibrated light source. The composition and thickness of the ALD films are measured on glass samples from the same deposition runs by profilometry and x-ray fluorescence calibrated by Rutherford backscattering. The absorption coefficient was determined by optical analysis based on ellipsometry measurements using a Woolam variable angle ellipsometer in the wavelength range 260–1700 nm at 65°, 70°, and 75° angle of incidence. The conductivity of the ALD ZTO films is too low to be measured with standard setups.

The device results for the different buffer layer processes are shown in Table I. For batch A, the KCN etched device A1 with ALD growth at 95 °C gives the highest efficiency, even higher than that for the CdS reference from the same anneal (Fig. 1). The spread among 6–8 devices on the same sample is small in J_{sc} and V_{oc} and slightly larger in FF. For batch B the spread in device performance is larger, mainly related to small areas of delamination in particular for some samples (B_{ref} and B1). These areas are excluded in further analysis as seen by the smaller number of cells (Table I). The device with ALD deposition at 120 °C shows almost equal performance as compared with the CdS

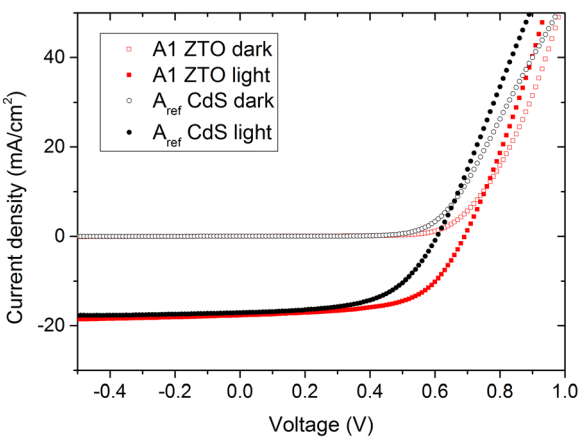

FIG. 1. IV curves of devices A_{ref} and A1; ZTO deposited at 95 °C.

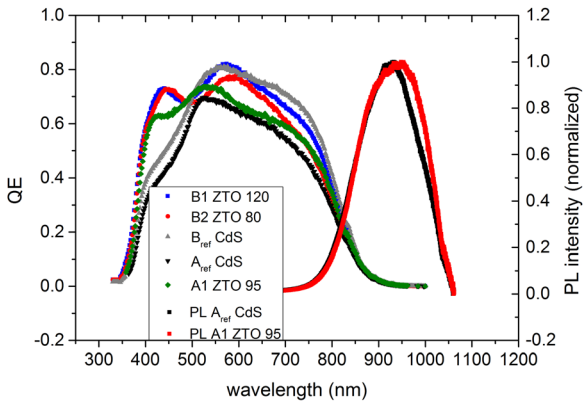

FIG. 2. EQE of all cells in Figs. 1 and 2 with normalized PL of devices A_{ref} and A1.

reference while the 80 °C sample gives high V_{oc} and J_{sc}, but with a clear loss in FF. Light-soaking under the class A solar simulator lamp was tested for the samples in batch A. An increase in FF is observed for some devices after 2 min, but then the effect saturates. The efficiency of the best device after 2 min is shown in Table I, but all other values are obtained without intentional light-soaking. One general difference between batches A and B is the overall higher short circuit current for batch B as seen both for CdS reference devices and ALD devices. From QE measurements (Fig. 2), the gain in J_{sc} is seen to originate from an increase over all wavelengths. The CdS reference device B_{ref} has both slightly higher V_{oc} and J_{sc} as compared with the first batch, giving efficiencies of up to 7.2%. This spread of CdS devices from our baseline process around 6%–7% in absolute efficiency is similar to previous results.[16]

From previous studies on CIGS it is shown that a ZTO buffer layer grown at 120 °C with a Sn/Sn + Zn composition of 0.2 leads to the same CBO as for CBD-CdS buffer layers.[9] This may explain the observation of similar V_{oc} values for samples B1 and B_{ref} assuming that the interface quality of the buffer layer systems is equal. The loss in FF for the 80 °C sample, with blocking of the forward current (Fig. 3), indicates barrier formation at the interface. This is compatible with the expected increase in conduction band level for this low deposition temperature film. Since optical characterization of ZTO deposited at 80 °C was not included in our previous work, ellipsometry measurements were performed on a glass sample, loaded together with B2 in the ALD reactor. The absorption edge clearly shifts to higher energy as compared with the higher deposition temperatures, but the edge is non-sharp. A band gap around 3.8–4.0 eV can be estimated from a Tauc plot for this 80 °C ZTO film. The energy band alignment with CIGS for ZTO films deposited at 90–180 °C is studied in Ref. 12 for 50 nm thick films. An increase in band gap from 3.49 eV to 3.74 eV is seen as temperature is decreased from 120 to 90 °C. This band gap increase is mainly expected to come from an increase in CBM, which implies that a gradual increase in CBM is expected from B1 (120 °C) to A1 (95 °C) to B2 (80 °C). On CZTS, B1 is expected to give a similar CBO to CdS, i.e., a cliff of around 0.3 eV.[5] Therefore, the CBO for A1 should be close to zero, while for B2 the CBM should be positive, with a spike around 0.1–0.3 eV. Measurements of the real band alignments of these interfaces are needed for further understanding. In addition, the influence of composition, doping, and buffer layer thickness needs to be clarified before an optimum ZTO buffer layer can be defined for CZTS.

Sample A1 yields higher performance compared with the CdS reference and thus, for further understanding of the recombination limitations, JVT measurements were performed as shown in Figure 4. A remarkable difference in the temperature dependence of V_{oc} can be seen. While the CdS reference device gives an activation energy of around 1 eV, similar to several of our previously reported CdS devices,[16,17] the V_{oc} of the ZTO device extrapolates to 1.36 eV at 0 K. The ideality factor was confirmed to be temperature-independent within the interval used for extrapolation.

Since an activation energy of 1.36 eV is still lower than the expected fundamental band gap of kesterite CZTS of around 1.5 eV, it might be concluded that the devices are still limited by interface recombination, but with a larger energy barrier for recombination. However, this activation energy is also compatible with dominant bulk recombination since the bulk radiative recombination energy in CZTS is in fact lower than 1.5 eV. This can be seen by room temperature PL measurements, which generally give a peak at 1.3–1.35 eV.

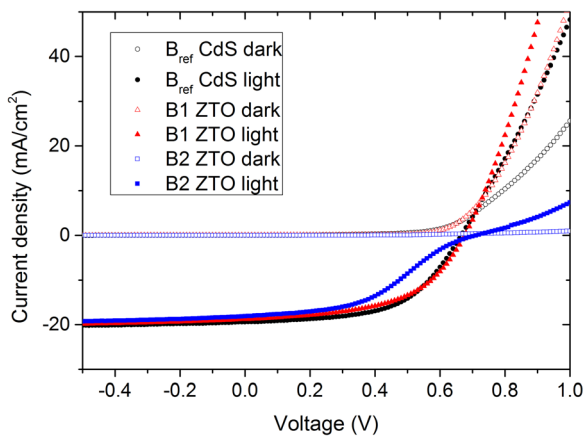

FIG. 3. IV curves of devices B_{ref}, B1, and B2; ZTO deposited at 120 °C and 80 °C.

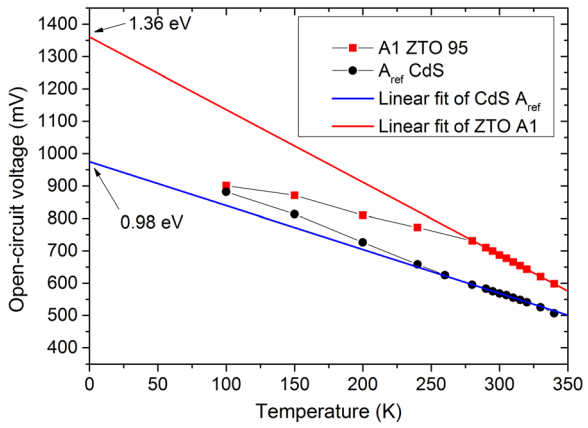

FIG. 4. V_{oc}(T) of A_{ref} (CdS) versus A1 (ZTO 95 °C). Within the linear region used for extrapolation, the ideality factor is confirmed to be temperature independent.

In our case, room temperature PL measurements (Fig. 2) of samples A_{ref} and A1 also give a PL peak at around 1.3–1.34 eV. Interpretation of PL data from CZTS must be done with caution since interference effects can distort the spectrum.[18] In this case, we have minimized the interference effect by using relatively thin CZTS absorber layers of around 800 nm. Larger thicknesses are often used for CZTS solar cells, but as we showed in a study of varying thickness, collection of minority carriers is limited in these materials, and no substantial gain could be seen by increasing thickness above around 750–1000 nm.[19]

The fact that bulk recombination in CZTS films occurs over an energy gap smaller than the fundamental kesterite band gap is another important (although separate) question. Recent work suggested that the reason for this is the existence of large spatial band gap fluctuations coming from high concentrations of Cu-Zn antisite disorder, which is thought to be prevalent in synthetic CZTS.[20] This results in localized band gap narrowing, seen as tailing that dominates radiative recombination and limits the voltage. Another possibility is segregation of secondary phases with lower band gaps.

Based on the aforementioned considerations and the coincidence of the activation energy from JVT with the energy of the PL peak, we interpret the increase in activation energy when using the ZTO buffer as a shift of the dominant recombination pathway away from the interface and into the CZTS bulk. This is an effect of the improved band alignment in the CZTS/ZTO cells.

This is different from our previous results using ALD Zn(O,S) buffer layers,[16] where lower activation energies are obtained, and where room temperature V_{oc} and device efficiency are always substantially lower than the CdS reference devices. In this case, increased V_{oc}, of up to 713 mV, as well as higher E_a are seen, clearly showing that a high quality interface both in terms of band alignment and interface formation is obtained using ALD ZTO buffer layers.

In conclusion, we have shown that the standard CdS buffer layer in CZTS solar cells can be replaced with a ZTO film deposited by atomic layer deposition. The open circuit voltage is higher for the ZTO buffer devices as compared with their CdS reference cells with a top efficiency after 2 min light-soaking of 7.4% without antireflective coating. JVT analysis shows an activation energy for recombination of 1.36 eV, which is close to the room temperature PL peak of these CZTS absorbers. This means that V_{oc} is either limited by bulk recombination, or that the barrier for interface recombination is increased. In any case, part of the interface recombination has been suppressed by changing buffer layer material, and ZTO is shown to be a superior junction material for CZTS as compared with CdS.

Funding from the Swedish Energy Agency, Swedish Research Council, Wallenberg Academy Fellows Program, and Foundation for Strategic Research is gratefully acknowledged. Olivier Donzel-Gargand is acknowledged for TEM analysis.

[1]K. Ito and T. Nakazawa, Jpn. J. Appl. Phys., Part 1 **27**(11), 2094–2097 (1988).
[2]H. Katagiri, Thin Solid Films **480–481**, 426–432 (2005).
[3]W. Wang, M. Winkler, O. Gunawan, T. Gokmen, T. Todorov, Y. Zhu, and D. Mitzi, Adv. Energy Mater. **4**(7), 1301465 (2014).
[4]B. Shin, O. Gunawan, Y. Zhu, N. A. Bojarczuk, S. J. Chey, and S. Guha, Prog. Photovoltaics **21**(1), 72–76 (2013).
[5]M. Bär, B. Schubert, B. Marsen, R. Wilks, S. Pookpanratana, M. Blum, S. Krause, T. Unold, W. Yang, L. Weinhardt, C. Heske, and H. W. Schock, Appl. Phys. Lett. **99**(22), 222105 (2011).
[6]C. Hages, N. Carter, R. Agrawal, and T. Unold, J. Appl. Phys. **115**(23), 234504 (2014).
[7]U. Rau and H. Schock, Appl. Phys. A **69**, 131–147 (1999).
[8]G. Brammertz, M. Buffiere, S. Oueslati, H. ElAnzeery, K. Messaoud, S. Sahayaraj, C. Köble, M. Meuris, and J. Poortmans, Appl. Phys. Lett. **103**, 163904 (2013).
[9]M. Kapilashrami, C. X. Kronawitter, T. Törndahl, J. Lindahl, A. Hultqvist, W. C. Wang, C. L. Chang, S. S. Mao, and J. H. Guo, Phys. Chem. Chem. Phys. **14**(29), 10154–10159 (2012).
[10]M. Morkel, L. Weinhardt, B. Lohmuller, C. Heske, E. Umbach, W. Riedl, S. Zweigart, and F. Karg, Appl. Phys. Lett. **79**(27), 4482–4484 (2001).
[11]J. Lindahl, C. Hagglund, J. T. Watjen, M. Edoff, and T. Törndahl, Thin Solid Films **586**, 82–87 (2015).
[12]J. Lindahl, J. Keller, O. Donzel-Gargand, P. Szaniawski, M. Edoff, and T. Törndahl, Sol. Energy Mater. Sol. Cells **144**, 684–690 (published online).
[13]T. Ericson, T. Kubart, J. J. Scragg, and C. Platzer-Bjorkman, Thin Solid Films **520**(24), 7093–7099 (2012).
[14]J. Lindahl, U. Zimmermann, P. Szaniawski, T. Törndahl, A. Hultqvist, P. Salome, C. Platzer-Bjorkman, and M. Edoff, IEEE J. Photovoltaics **3**(3), 1100–1105 (2013).
[15]A. Hultqvist, C. Platzer-Bjorkman, U. Zimmermann, M. Edoff, and T. Törndahl, Prog. Photovoltaics **20**(7), 883–891 (2012).
[16]T. Ericson, J. Scragg, A. Hultqvist, T. Wätjen, P. Szaniawski, T. Törndahl, and C. Platzer-Björkman, IEEE J. Photovoltaics **4**(1), 465–469 (2014).
[17]J. Scragg, T. Ericson, X. Fontane, V. Izquierdo-Roca, A. Perez-Rodriguez, T. Kubart, M. Edoff, and C. Platzer-Björkman, Prog. Photovoltaics **22**(1), 10 (2014).
[18]J. K. Larsen, S. Y. Li, J. J. S. Scragg, Y. Ren, C. Hagglund, M. D. Heinemann, S. Kretzschmar, T. Unold, and C. Platzer-Bjorkman, J. Appl. Phys. **118**(3), 035307 (2015).
[19]Y. Ren, J. Scragg, C. Frisk, J. Larsen, S.-Y. Li, and C. Platzer-Björkman, "Influence of the Cu_2ZnSnS_4 absorber thickness on thin film solar cells," Phys. Status Solidi A (published online).
[20]J. Scragg, J. Larsen, M. Kumar, C. Persson, J. Sendler, S. Siebentritt, and C. Platzer-Björkman, "Cu-Zn disorder and band gap fluctuations in $Cu_2ZnSn(S,Se)_4$: Theoretical and experimental investigations," Phys. Status Solidi B (published online).